International Scholarly Research Network
ISRN Renewable Energy
Volume 2012, Article ID 939878, 5 pages
doi:10.5402/2012/939878

*Research Article*

# Computational Analysis of 30 Kw Contra Rotor Wind Turbine

**P. Santhana Kumar,[1] R. Joseph Bensingh,[1] and A. Abraham[2]**

[1] *Arstps, Central Institute of Plastic Engineering and Technology, Chennai 600032, India*
[2] *SERC, CSIR, Chennai 600113, India*

Correspondence should be addressed to P. Santhana Kumar, kumarpsk@yahoo.co.in

Received 20 February 2012; Accepted 11 April 2012

Academic Editors: A. Bosio, S. Li, and S. Rehman



The aim of this study is to optimize and analyze the characteristics of the upwind primary rotor and the downwind secondary rotor of the contra rotor wind turbine to increase the aerodynamic performance by using computational fluid dynamic (CFD). The main objective is to provide maximum energy that can be extracted by the primary and secondary rotor from the renewable resource of wind to increase the thrust power. For this purpose, two kinds of rotor configurations which are 3-bladed single and 3-bladed contra-rotating rotor were compared by using CFD. The results of the primary and secondary rotor are validated with measurements of the 30 KW Contra rotor wind turbine available on literature and plotted for power output. The optimum axial distance between the two rotors are investigated through CFD for increased performance. In addition, the increased thrust and torque for each rotor configuration are compared for aerodynamic feasibility.

## 1. Introduction

Wind power is a significant promising source of renewable energy, and its conversion to usable energy is important considering the rapid decrease of fossil energy sources of earth. In order to obtain energy from wind, a lot of wind turbines are being constructed [1–3]. However, regions having high wind energy density are finite [4]. Therefore, different research has been conducted on how to optimize the behavior of wind power units. Some researchers concentrated mainly on the simulation of the performance of the horizontal wind turbine of single rotors using commercial software. Others made a comparison between theoretical and experimental work in the field. Generally, single rotor wind turbines (SRWT) are used for conventional wind turbine systems. According to Betz theory [5], the maximum energy conversion efficiency of conventional wind turbines having a single rotor is about 59%. But the maximum efficiency obtained by contra rotors having the same area is increased to 64% [6]. Based on these studies, in order to increase the power efficiency of wind turbines on contra-rotating wind turbines (CRWT) that have two rotors rotating in opposite direction coaxially have been carried out [7–15]. These studies are based on the various wind turbine energy assessments and comparison of power output in CRWT with that of SRWT. In the present studies, a comparison of 30 kW CRWT with SRWT is made using CFD prediction on power output (kW), thrust (N), and torque (N-m) for each rotor configurations (3-blade, 3-blade contra), and the aerodynamic improvement of a CRWT was considered.

## 2. Operation of CRWT

A contra-rotating wind turbine (CRWT) can be described as a system consisting of two rotors separated by an appropriate distance. One of the rotors is rotating in counter-clockwise direction and the other in clockwise direction. The primary rotor is characterized by a counter-clockwise rotation in upwind location, while the secondary rotor is characterized by a clockwise rotation in downwind location. The secondary rotor is advisable to rotate in the same direction as the wake in order to extract the available energy in the wake efficiently. CRWT is more feasible for less density areas of wind energy and also it accounts to less moment in the turbine towers due to torque equivalence of both rotors.

## 3. CFD Method

The physical aspects of any fluid flow are governed by three fundamental principles.

(1) Mass is conserved.

(2) Newton's second law of momentum (Force = mass × acceleration).

(3) Energy is conserved.

These fundamental physical principles can be expressed in terms of basic mathematical equations, which in their most general form are either integral equations or partial differential equations. Computational fluid dynamics is the art of replacing the integrals or the partial derivatives (as the case may be) in these equations with discretized algebraic forms, which in turn are solved to obtain numbers for the flow field values at discrete points in time and/or space. The end product of CFD is indeed a collection of numbers, in contrast to a closed-form analytical solution. However, in the long run, the objective of most engineering analyses, closed form or otherwise, is a quantitative description of the parameters.

*3.1. Governing Equations.* The mathematical equations describing the aerodynamics of wind turbines [16] are based on the equations of conservation of mass and momentum together with other additional equations for the turbulence. The standard $k$-$\boldsymbol{\varepsilon}$ turbulence model is used in this study. The equations for the turbulent kinetic energy $k$ and the dissipation rate of the turbulent kinetic energy $\boldsymbol{\varepsilon}$ are solved. The time averaged gas phase equations for steady turbulent flow are [16]

$$\frac{\partial}{\partial x_i}(\rho u_i\, \Phi) = -\frac{\partial}{\partial x_i}\left(\Gamma_\Phi\, \frac{\partial \phi}{\partial x_i}\right) + S_\Phi, \tag{1}$$

where $\boldsymbol{\varphi}$ is the dependent variable that can represent the velocity $u_i$, $k$ is the turbulent kinetic energy, $\mathbf{s}_{\boldsymbol{\varphi}}$ is the source term, and $\boldsymbol{\varepsilon}$ is the dissipation rate of the turbulent kinetic energy.

*(a) Continuity Equation.* The equation of conservation of mass or continuity equation is given by [16]

$$\frac{\partial}{\partial x_i}(\rho \tilde{u}_i) = 0, \tag{2}$$

where, "$\rho$" is the density of air.

*(b) Momentum Equation.* The momentum equation is given by [16]

$$\rho\left[\frac{\partial \tilde{u}_i}{\partial t} + \frac{\partial \tilde{u}_i \tilde{u}_j}{\partial x_j}\right] = -\frac{\partial \tilde{p}}{\partial x_i} + \frac{\partial}{\partial x_j}\left(\mu \frac{\partial \tilde{u}_i}{\partial x_j}\right) + \rho g \beta\left(T_{\text{ref}} - \tilde{t}\right). \tag{3}$$

Table 1: CRWT and SRWT model specifications.

| Specifications | Primary rotor | Secondary rotor |
|---|---|---|
| No. of blades | 3 | 3 |
| Rotor diameter | 5.5 m | 11 m |
| Rotor position | Upwind | Downwind |
| Airfoil | NACA 4415 | NACA 0012 |
| Rotation | Clockwise | Counter-Clockwise |
| Built-in twist (°) | 0° | −2° |

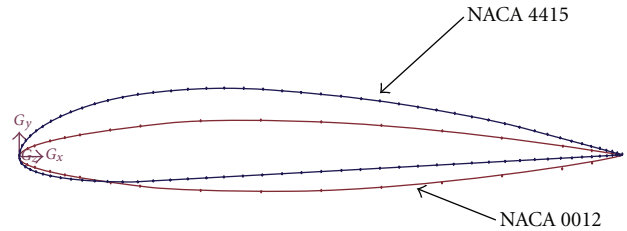


Figure 1: Blade profile of CRWT.

*(c) Energy Equation.* The energy equation is given by [16]

$$\rho\left[\frac{\partial C_p \tilde{t}}{\partial t} + \frac{\partial C_p \tilde{u}_i \tilde{t}}{\partial x_j}\right] = \frac{\partial}{\partial x_j}\left(k \frac{\partial \tilde{t}}{\partial x_j}\right) + \tilde{S}_t. \tag{4}$$

The instantaneous quantity $\tilde{\phi}$ can be expressed as follows: $\tilde{\phi} = \Phi + \phi$, where $\Phi$ is the time averaged value and $\phi$ is fluctuating part, this is know as Reynolds decomposition. After substituting the above relation we obtain Reynolds-averaged Navier-Stokes equations (RANS). And the RANS have the form [16]

$$\begin{aligned} \frac{\partial}{\partial x_i}(\rho U_i) &= 0, \\ \rho\left[\frac{\partial U_i}{\partial t} + \frac{\partial U_i U_j}{\partial x_j}\right] &= -\frac{\partial P}{\partial x_i} + \frac{\partial}{\partial x_j}\left(\mu \frac{\partial U_i}{\partial x_j} - \rho \overline{u_i u_j}\right) \\ &\quad + \rho g \beta (T_{\text{ref}} - T). \end{aligned} \tag{5}$$

The unknowns $\rho\overline{u_i u_j}, \rho\overline{u_j t}$ are called Reynolds stress and velocity temperature correlation, respectively. The whole problem in the RANS arises due to these two terms, which is also called as turbulence closure problem.

## 4. CAD Modelling of Contra Rotar

In order to predict the performance of a CRWT, initially single rotor wind turbine is modeled with NACA series aerofoil with the specification of primary rotor and then the contra rotor wind turbine is also modeled as per the specification as given in Table 1 with parametrical optimization on axial distance between the two rotors and diameter ratio (primary/secondary rotor).

The CAD model contains the full geometry of the CRWT which is nacelle or hub, the primary, and secondary rotor. The blade geometry itself is based on a set of 2D profiles of NACA-0012 and NACA-4415 as shown in Figure 1 for both

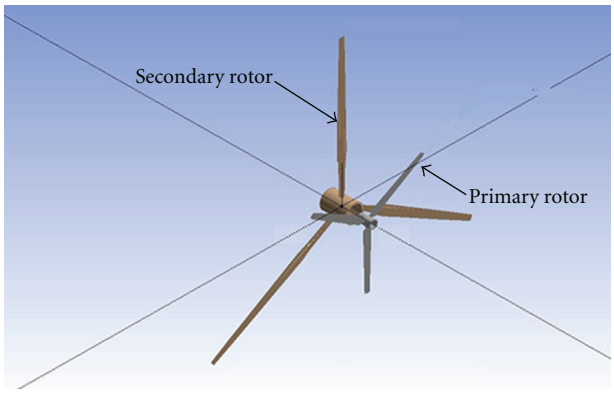


Figure 2: Geometry model of CRWT.

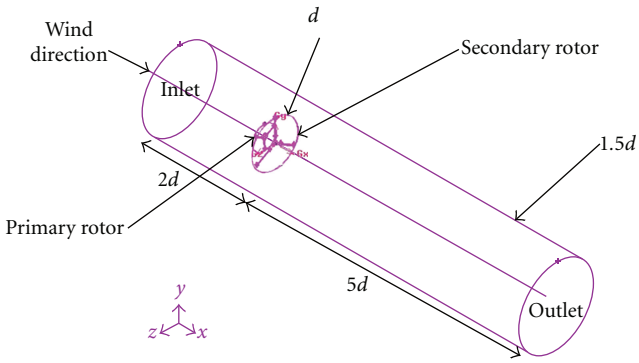


Figure 3: Cylindrical domain of CRWT.

the rotors that enable it to give aerodynamic representation of the relevant structure. The following 3D model with the constraints is generated using CAD software. The upwind Primary rotor and downwind Secondary rotor is developed with the given specification of optimized diameter ratio and axial distance with built-in twist ($-2^\circ$) of NACA0012-NACA4415 aerofoil coordinates to a scale of 1 : 1 as shown in Figure 2.

## 5. Computational Analysis

The developed model of contra rotor wind turbine is imported to CFD. The equation of fluid flow is usually solved in stationary (or inertial) reference frames. However, there are many fluid flow problems that require the equations to be solved in a moving (or noninertial) reference frames. Rotating rotor of wind turbine is such a case of moving reference frame (MRF). The computational domain is extended in axial direction roughly to predict the flow characteristics in the upstream of $2d$ from the rotor and in the downstream of $5d$ from the rotor in terms of rotor diameter ($d$) as shown in Figure 3. In the vertical plane of the rotor, the cylindrical domain diameter is $5d$ of the rotor diameter ($d$) to capture the wake behavior of the upwind and downwind of the rotor. The developed computational domain is meshed with tetrahedral elements with appropriate interval size of elements in to 1120000 cells as shown in Figure 4.

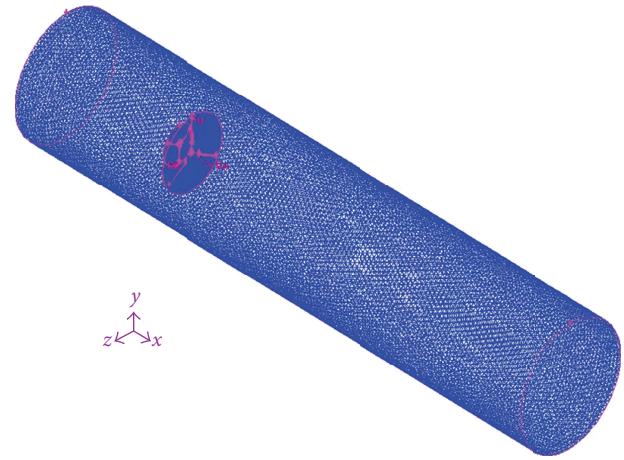


Figure 4: Meshed domain of CRWT.

## 6. Results and Discussion

*6.1. Validation of CFD Method.* To validate the results based on CFD, the power output (kW) as given in Jung et al [7] for the 30 kW CRWT is computed and compared to measured values [7]. The CRWT system has 3 blades of 5.5 m diameter primary rotor and 11.0 m diameter secondary rotor. The comparison of the power output (kW) versus wind speed is shown in Figure 5 for SRWT and CRWT. In SRWT for wind speed up to 6 m/s computationally calculated results approximately agree with the measured values [7] and after 6 m/s variation are predicted due to the extension bar provided for some distance in SRWT-CFD model comparing the experimental model. In CRWT for wind speed up to 14 m/s computationally calculated results agree well with the measured values [7] and the maximum power output of 90 kW is predicted at 14 m/s.

*6.2. Parametric Investigation of CRWT.* The wind flow approaching the upwind primary rotor and downwind secondary rotor should be taken in to consideration for obtaining high-power output and aerodynamic feasibility. In this case, the relative size of diameter ratio 1 : 2 is fixed as the power increase amounts to 20% [7] as well as the appropriate axial distance between the two rotors should be predicted for high-power output that extract more energy from the wind than SRWT. Leading to the objective, parametric investigations are carried out for $0.25d$, $0.5d$, $0.65d$, and $0.75d$ ($d$-primary rotor diameter) to predict the optimum axial distance between the two rotors. The effects of axial distance between the two rotors on the increase of power in terms of percentage are shown in Figure 6. In CRWT for wind speed at 10 m/s computationally calculated power increase of 8.9% at $0.5d$ agree with the measured values [7] but before $0.5d$ variations are seen due to less wake energy extraction by secondary rotor and the maximum power increase of 9.67% is computationally predicted at 10 m/s at $0.65d$. Above $0.65d$ of axial distance between the two rotors the power increase of CRWT is reduced to 7.8% at 0.75d due to the less energy extraction from the wake of the primary rotor.

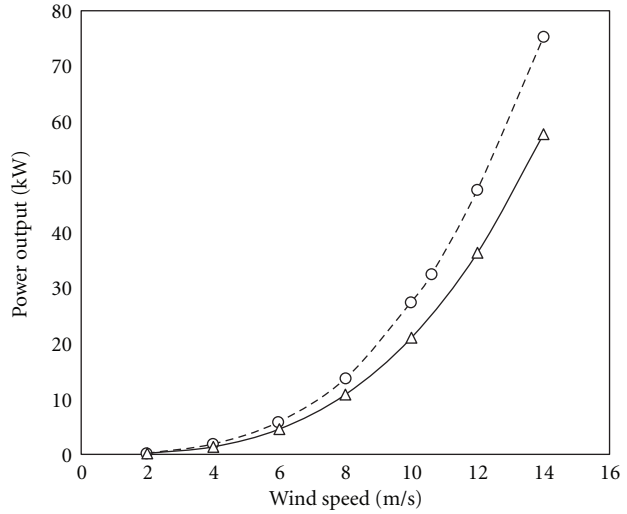


(a)

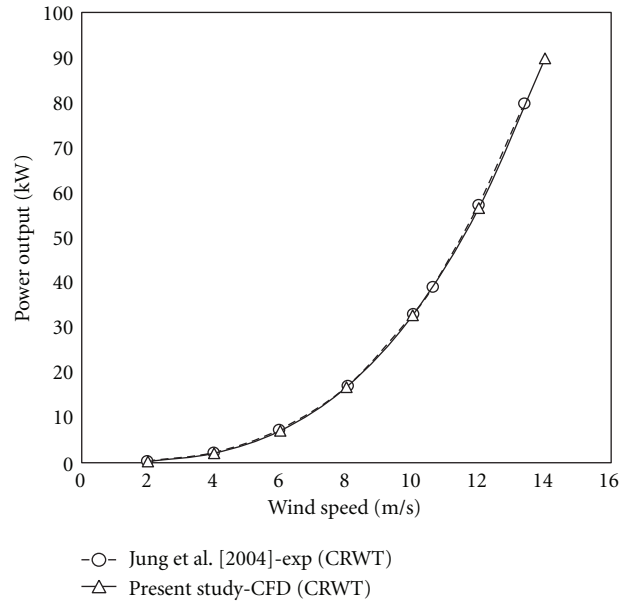


(b)

Figure 5: Power output (kW) versus wind speed (m/s) for SRWT and CRWT.

*6.3. Performance Comparison of SRWT and CRWT.* For the aerodynamic performance prediction of a CRWT, two kinds of rotor configurations were compared by using CFD. One is a single rotor having three blades and another is a 3-bladed contra-rotating rotor, as shown in Figure 3. It has two rotors rotating in opposite direction along the same axis. Thrust (N) curve for SRWT and CRWT for various wind speed from 2 (m/s) to 14 (m/s) are plotted in the interval of 2 (m/s) as shown in Figure 7. The thrust computationally obtained for SRWT is 350 N and CRWT is 545 N at 10 m/s which resembles 35% thrust increase in CRWT than SRWT. In CRWT with addition of secondary rotor with predicted 0.65$d$ axial distance and diameter ratio of 1 : 2, the thrust increases and the linearly steep thrust curve is obtained. Torque (N-m) curve for SRWT and CRWT for various wind speed up to 14 (m/s) are plotted as shown in Figure 8. The maximum torque computationally obtained is 4770 N-m at 14 m/s for CRWT which is more than the torque obtained at the same wind speed for SRWT. The steep torque curve determines the performance increment in CRWT and a maximum increase of 20.75% torque performance is computationally obtained for aerodynamic feasibility.

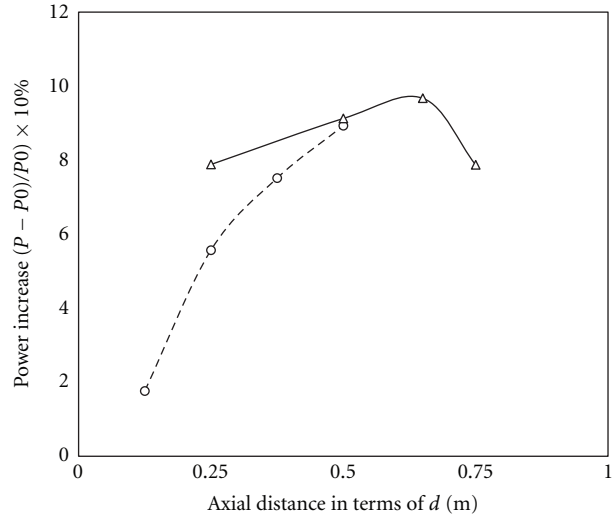


Figure 6: Power increase ((*P*−*P0*)/*P0* ×100%) versus axial distance (*d*).

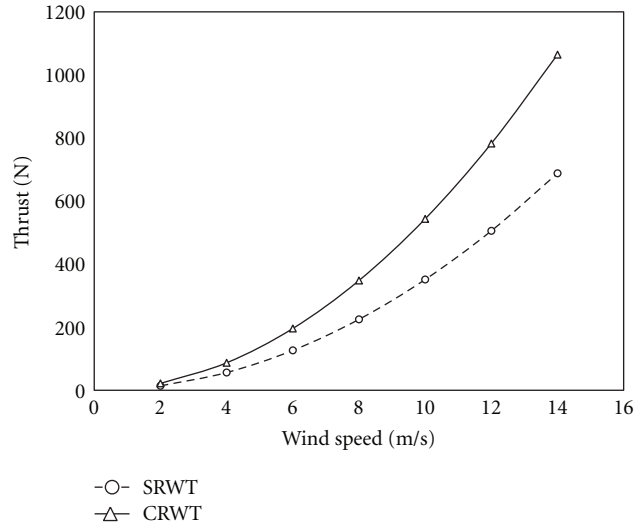


Figure 7: Thrust (N) versus wind speed.

## 7. Conclusion

The aerodynamic performance analysis has been carried out for 30 KW CRWT by using computation fluid dynamics

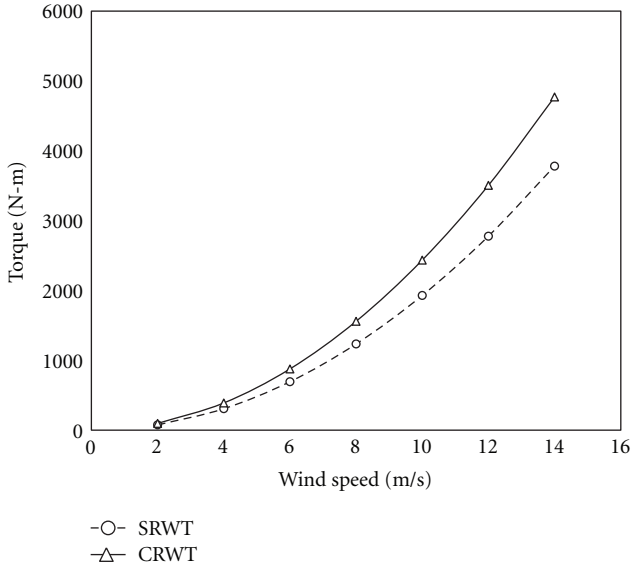


Figure 8: Torque (N-m) versus wind speed.

and was validated with measured values. The calculated power output of CRWT was found to be in good agreement with the experimental results and maximum power output of 90 kW is obtained at 14 m/s. The appropriate diameter ratio of CRWT were considered and the appropriate axial distance is computationally calculated at 0.65$d$, where the maximum power increase of 9.67% is obtained which is more than the measured values at 0.5$d$. The thrust computed produces linearly steep curve with the 35% increment in thrust for CRWT than SRWT for the same wind speed at 10 m/s. It is found that the torque was maximum in CRWT comparing SRWT with addition of secondary rotor and the increased torque performance of 20.75% for CRWT was achieved when the axial distance is 0.65$d$. Approximately good correlation between the computational and measured results was obtained. Based on the computational results, the CRWT is to be fairly effective in extracting energy from the wind where the less density of wind energy is found.

## Acknowledgments

This work has been supported by the SERC (Structural Engineering Research Centre)-CSIR and ARSTPS (Advance Research School for Technology and Product Simulation)-CIPET.

## References

[1] S. Mathew, *Wind Energy Fundamentals, Resource Analysis and Economics*, Springer, New York, NY, USA, 2006.

[2] I. Ushiyama, "Small wind turbines in sustainable urban environment," Urban Planning-Sustainable Cities in the Framework of the German in Japan, 2005.

[3] Lahmeyer International GmbH, "Zafarana KfW IV wind farm," Project Design Document (CDM PDD), Version 03.1, 2008.

[4] IS-875, (Part 3-wind loads), (reaffirmed 2003), Bureau of Indian Standards, 1987.

[5] J. F. Manwell, J. G. McGowan, and A. L. Rogers, *Wind Energy Explained, Theory, Design and Application*, John Wiley & Sons, New York, NY, USA, 2002.

[6] B. G. Newman, "Actuator-disc theory for vertical-axis wind turbines," *Journal of Wind Engineering and Industrial Aerodynamics*, vol. 15, no. 1–3, pp. 347–355, 1983.

[7] S. N. Jung, T. S. No, and K. W. Ryu, "Aerodynamic performance prediction of a 30 kW counter-rotating wind turbine system," *Renewable Energy*, vol. 30, no. 5, pp. 631–644, 2005.

[8] K. Appa, "Energy Innovations Small Grant (EISG) program (Counter Rotating Wind Turbine System)," EISG Final Report, EISG, Lake Forest, Calif, USA, 2002.

[9] W. Z. Shen, V. A. K. Zakkam, J. N. Sørensen, and K. Appa, "Analysis of counter-rotating wind turbines," *Journal of Physics*, vol. 75, no. 1, Article ID 012003, 2007.

[10] I. Ushiyama, T. Shimota, and Y. Miura, "Experimental study of the two-staged wind turbines," *Renewable Energy*, vol. 9, no. 1–4, pp. 909–912, 1996.

[11] C. Lindenburg, "Investigation into rotor blade aerodynamics—analysis of the stationary measurements on the UAE phase-VI rotor in the NASA-Ames wind tunnel," Tech. Rep. ECN-C-03-025, 2003.

[12] D. E. Neff and R. N. Meroney, "Mean wind and turbulence characteristics due to induction effects near wind turbine rotors," *Journal of Wind Engineering and Industrial Aerodynamics*, vol. 69–71, pp. 413–422, 1997.

[13] Y. Himri, S. Rehman, B. Draoui, and S. Himri, "Wind power potential assessment for three locations in Algeria," *Renewable and Sustainable Energy Reviews*, vol. 12, pp. 2488–2497, 2008.

[14] S. Rehman and N. M. Al-Abbadi, "Wind shear coefficient, turbulence intensity and wind power potential assessment for Dhulom, Saudi Arabia," *Renewable Energy*, vol. 33, no. 12, pp. 2653–22660, 2008.

[15] S. Rehman, I. M. El-Amin, F. Ahmad, S. M. Shaahid, A. M. Al-Shehri, and J. M. Bakhashwain, "Wind power resource assessment for Rafha, Saudi Arabia," *Renewable and Sustainable Energy Reviews*, vol. 11, no. 5, pp. 937–950, 2007.

[16] J. Tu, *Computational Fluid Dynamics—A Practical Approach*, Elsevier, Amsterdam, The Netherlands, 2008.